Available online at www.sciencedirect.com
SCIENCE DIRECT

Journal of the European Ceramic Society 23 (2003) 1193–1197
www.elsevier.com/locate/jeurceramsoc

Hertzian contact damage in a highly porous silicon nitride ceramic

Jihong She[a,*], Jian-Feng Yang[a], Yoshihisa Beppu[b], Tatsuki Ohji[a]

[a]*Synergy Materials Research Center, National Institute of Advanced Industrial Science and Technology (AIST), Nagoya 463-8687, Japan*
[b]*Synergy Ceramics Laboratory, Fine Ceramics Research Association (FCRA), Nagoya 463-8687, Japan*

Received 31 March 2002; received in revised form 30 August 2002; accepted 7 September 2002

Abstract

Hertzian indentation tests were performed to evaluate the contact damage behavior of a highly porous Si_3N_4 ceramic. Using a bonded-interface technique, the Hertzian contact damage patterns were examined. As a result of intragranular microfracture under Hertzian contact, a distributed subsurface damage region is developed beneath the indenter. It was found that the damage region extends progressively with increasing contact load. In strength tests, failures were observed to originate from Hertzian indentation sites, giving rise to a gradual strength degradation.

Keywords: Contact damage; Porosity; Si_3N_4; Strength; Indentation

1. Introduction

Porous Si_3N_4 ceramics with high porosities (>30%) have been considered as one of the most favorable candidates for hot gas filtration in diesel exhaust systems or in the coal-gasification-generation process in order to limit the emission of some corrosive or toxic particles into the environment. In these applications, the surfaces of porous Si_3N_4 ceramics are subjected to continuous impact of solid particles. This may lead to localized damage and consequently to strength degradation or ultimately to catastrophic failure. Therefore, it is necessary to investigate the contact damage behavior of porous Si_3N_4 ceramics. As an effective technique under laboratory conditions, Hertzian indentation has been used to investigate the microstructural causes of contact damage in a variety of high-density ceramics.[1–9] Recently, several investigations have been directed toward the Hertzian contact damage behavior of porous alumina ceramics.[10–12] It has been shown that an increase in porosity may induce a brittle-plastic transition. This indicates that pores may play a critical role in the contact damage process. However, the specific mechanisms of Hertzian contact damage in porous ceramics are not well understood.

In the present work, Hertzian tests were conducted on a highly porous Si_3N_4 ceramic to reveal the contact damage mechanisms in porous ceramics. Furthermore, the strength of indented specimens was determined as a function of contact load to explore the mechanical response of such a porous Si_3N_4 ceramic under contact damage conditions.

2. Experimental procedure

A powder mixture of 95 wt.% α-Si_3N_4 (0.5 μm, E10, Ube Industries, Tokyo, Japan) and 5 wt.% Yb_2O_3 (High Purity Chemetals, Saitama, Japan) was ball-milled in methanol for 24 h, using high-purity Si_3N_4 media. After drying in a rotary evaporator and sieving through a 150-μm screen, the powders were compacted by die-pressing at a pressure of 10 MPa. Sintering was performed in a graphite resistance furnace at 1800 °C for 2 h under a N_2-pressure of 0.5 MPa. Subsequently, the sintered compacts were machined into rectangular specimens of 36 mm (length)×4 mm (width)×3 mm (thickness),

* Corresponding author. Tel.: +81-52-739-0135; fax: +81-52-739-0136.
E-mail address: jihong-she@aist.go.jp (J. She).

0955-2219/03/$ - see front matter © 2002 Elsevier Science Ltd. All rights reserved.
PII: S0955-2219(02)00301-1

where one surface perpendicular to thickness was polished to a 1-μm finish.

Porosity was calculated from the bulk density and the theoretical density, where the former was measured by a water-displacement method and the latter was estimated by the rule of mixtures. Flexural strength was determined by a three-point bending test at a support distance of 30 mm and a cross-head speed of 0.5 mm/min, with the polished surface as the tension side. To obtain the average strength, 10 specimens were tested. Young's modulus and Poisson's ratio were determined by the pulse-echo method. Vickers hardness was measured at a load of 98 N. These properties are summarized in Table 1. Microstructures were observed by scanning electron microscopy (SEM).

Hertzian indentation tests were performed in air with a universal testing machine at a constant cross-head speed of 0.5 mm/min over a load range of 100–2000 N, using tungsten carbide spheres of radius $r = 1.67$ mm. At each load, five specimens were indented. To facilitate the measurements of contact radius a at a given load P, the polished surfaces were coated with gold before indentation. On the other hand, the retained strengths of the indented specimens were tested under the same conditions as those of the unindented ones, with the indentation sites centered on the polished tensile surfaces. All broken specimens were examined to locate the origins of failure from indentations or extraneous flaws.

Subsurface contact damage was inspected using a "bonded-interface" technique.[2,3] Particularly, the polished surfaces of two specimens were bonded together with an adhesive. After the top surface was polished to a 1-μm finish with a diamond suspension, indentations were made along the interface trace. Then, the bonded specimens were separated and cleaned by dissolving the adhesive in acetone. Finally, the top and side surface were viewed by optical microscope.

Table 1
Physical properties of a porous Si_3N_4 ceramic

Porosity (%)	Strength (MPa)	Modulus (GPa)	Poisson's ratio	Hardness (GPa)
37.1	135	149	0.23	1.9

3. Results and discussion

Fig. 1 shows the surface view of a specimen after indentation at a load of 2000 N. As can be seen, well-defined impression and surface depression are developed under Hertzian contact. Based on the measurements of contact radii a from the residual impressions on the gold-coated surfaces, the relative indentation strain (a/r) and the mean indentation stress ($P/\pi a^2$) were calculated. The results are plotted in Fig. 2. For reference, an ideally elastic stress–strain response is also shown in Fig. 2 as a dashed line. It is obvious in Fig. 2 that the experimental data deviate distinctly from Hertzian elastic response. This indicates a high "plasticity" of the specimens under Hertzian indentation. On the other hand, it is worth to note in Fig. 2 that the indentation stress is almost constant over the entire strain range, in contrast to an increasing stress with strain for high-density Si_3N_4 ceramics.[13,14]

Fig. 3 shows the top-surface and side-section views of the specimens, which were indented in air using the bonded-interface technique with a 1.67-mm radius WC sphere at three different loads. As can be seen, the surface depression is accompanied by a distinct subsurface damage, which develops progressively with increasing load. At a load of 250 N, the damage is slight and is confined within a near-semispherical region below the contact circle. After indentation at $P = 1000$ N, the damage region has noticeably expanded, but still remains its hemisphericity beneath the contact area.

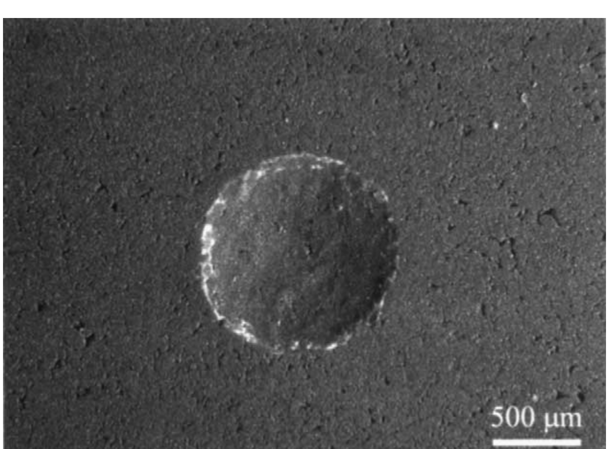

Fig. 1. Optical micrograph of surface damage in a specimen after Hertzian indentation at a load of 2000 N.

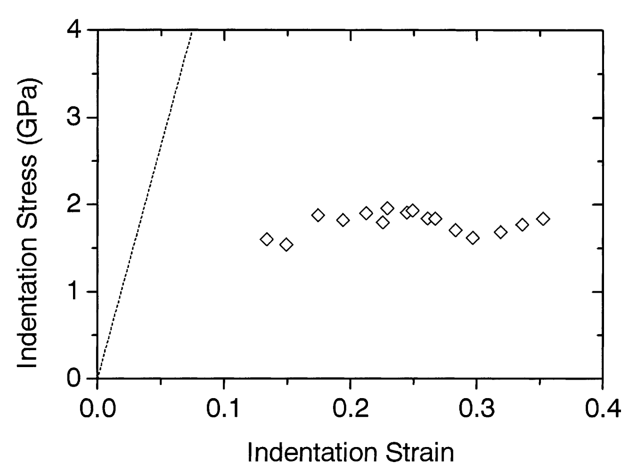

Fig. 2. Indentation stress–strain curve for a highly porous Si_3N_4. Dashed line is Hertzian elastic response.

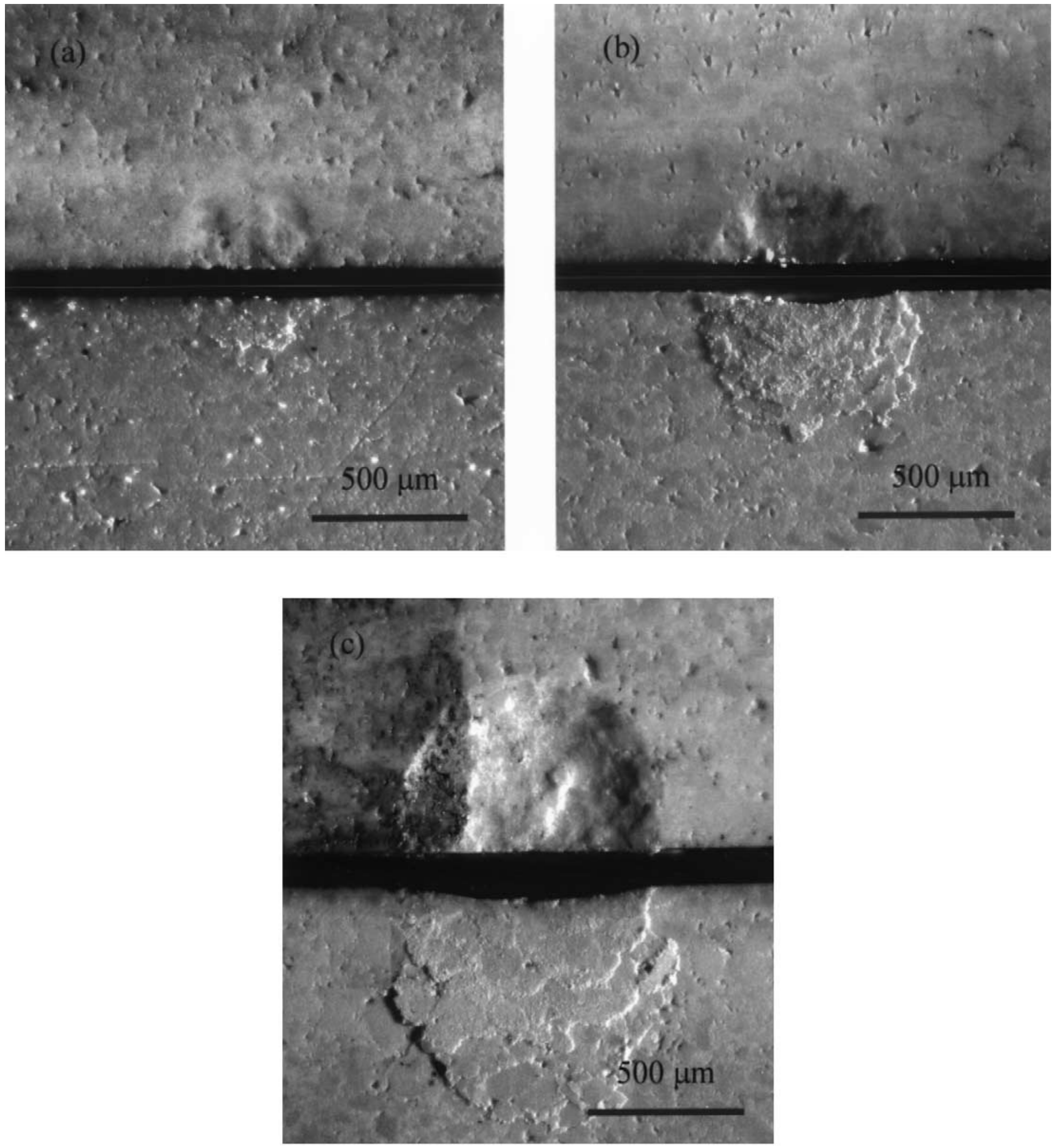

Fig. 3. Optical micrographs showing surface (top) and subsurface (bottom) damage in the specimens after indentation with a 1.67-mm radius WC sphere at loads: (a) $P=250$ N, (b) $P=1000$ N, and (c) $P=1500$ N.

When the indentation load is increases to 1500 N, the extended subsurface damage region departures significantly from an essentially hemispherical geometry, analogous to the observed contact-damage pattern in a micaceous glass-ceramic.[13] Therefore, one may infer that the above-mentioned plasticity of the specimens is a result of indentation damage in the subsurface region. To reveal the microstructural features of this contact damage, a high-magnification SEM observation was conducted on the subsurface damage region beneath the indenter. Fig. 4 compares the microstructures of the subsurface damage and undamaged regions. It is clear in Fig. 4 that most rod-like Si_3N_4 grains are fractured under Hertzian contact, giving rise to pore collapse. This implies that the plasticity of porous Si_3N_4 is probably due to intragranular microfracture. Mechanistically, the contact stress on the grains beneath the indenter increases with the indentation load until a critical value is achieved, causing a microfracture event. Once the grains fracture, the debris would be compacted within the pores, as shown in Fig. 4(b). In this case, the indentation load may be transferred to more neighboring grains, leading to a decrease in the contact stress on these grains. Due to the progressive increase in the load, however, the stress would increase again until another microfracture event occurs. This process is repeated so that the subsurface damage region extends gradually, as shown in Fig. 3. Since the onset of intragranular fracture is determined by the mechanical strength of the grains,[15] the contact stress at each microfracture event is

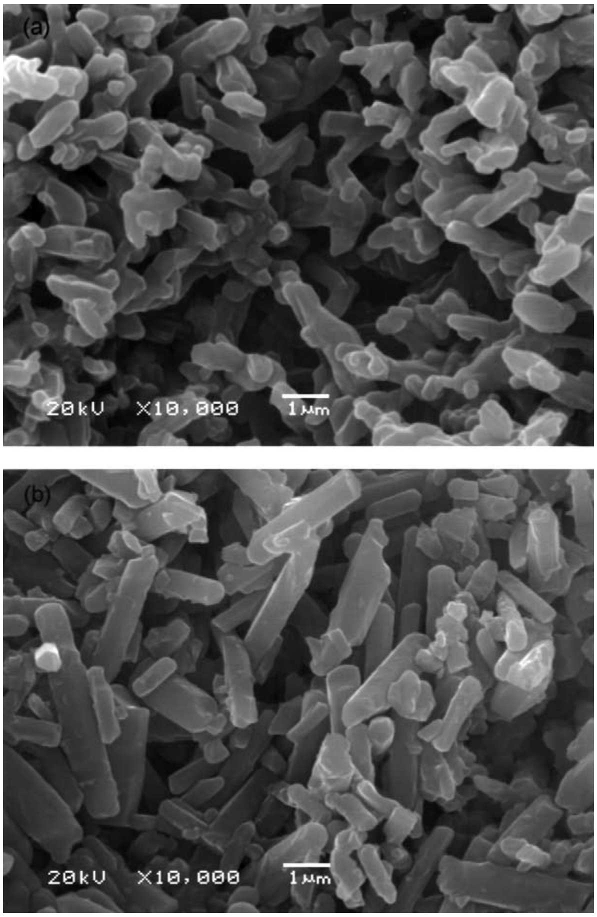

Fig. 4. High-magnification SEM views of (a) an undamaged region and (b) a damaged region beneath the indenter.

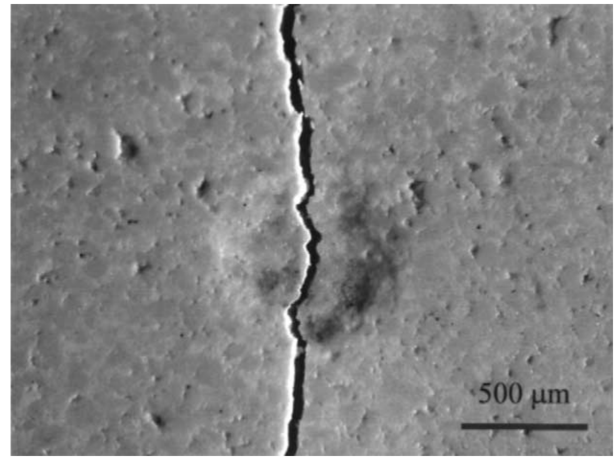

Fig. 5. Surface view of a specimen, which was indented at 750 N with a 1.67-mm radius WC sphere and then fractured in three-point bending.

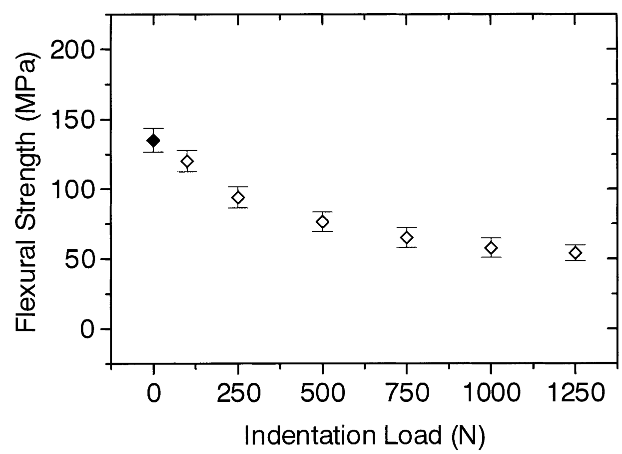

Fig. 6. Flexural strength as a function of indentation load. Open symbols indicate failure from indentation, closed symbols from other flaws.

expected to remain constant. This may account for the horizontal stress–strain curve in Fig. 2, because the indentation stress is directly proportional to the contact stress.[2]

Fig. 5 reveals the failure site of a contact-damaged specimen in strength test. Evidently, the fracture traverses the surface impression almost orthogonally, indicating a fracture origin within the subsurface damage region. Since the damage region extends progressively with increasing contact load, a gradual strength degradation is expected. Indeed, the strength was observed to decrease gradually with increasing load, as shown in Fig. 6.

4. Conclusions

The contact damage behavior of a highly porous Si_3N_4 ceramic was investigated as a function of indentation load. Using a bonded-interface technique, the surface and subsurface damage morphologies were inspected. It has been shown that intragranular microfracture occurs under Hertzian contact, giving rise to a distributed subsurface damage region beneath the indenter. This damage mechanism is responsible for the plasticity in porous Si_3N_4. On the other hand, the subsurface damage region was observed to extend progressively with increasing contact load, leading to a gradual strength degradation.

Acknowledgements

This work has been supported by METI as part of the Synergy Ceramics Project. The authors are members of the Joint Research Consortium of Synergy Ceramics. J.S. wishes to thank JISTEC for a financial support during his stay at Synergy Materials Research Center, AIST, Japan.

References

1. Makino, H., Kamiya, N. and Wada, S., Effects of grain size of hot-pressed silicon nitride on contact damage morphology and residual strength. *J. Am. Ceram. Soc.*, 1991, **74**, 2001–2004.
2. Guiberteau, F., Padture, N. P. and Lawn, B. R., Effect of grain size on hertzian contact damage in alumina. *J. Am. Ceram. Soc.*, 1994, **77**, 1825–1831.
3. Cai, H., Kalceff, M. A. S. and Lawn, B. R., Deformation and fracture of mica-containing glass-ceramics in hertzian contact. *J. Mater. Res.*, 1995, **9**, 762–770.
4. Xu, H. H. K., Wei, L., Padture, N. P., Lawn, B. R. and Yeckley, R. L., Effect of microstructural coarsening on hertzian contact damage in silicon nitride. *J. Mater. Sci.*, 1995, **30**, 869–878.
5. Pajares, A., Guibertuau, F., Lawn, B. R. and Lathabai, S., Hertzian contact damage in magnesia-partially-stabilized zirconia. *J. Am. Ceram. Soc.*, 1995, **78**, 1083–1086.
6. Padture, N. P. and Lawn, B. R., Contact fatigue of a silicon carbide with a heterogeneous grain structure. *J. Am. Ceram. Soc.*, 1995, **78**, 1431–1438.
7. Liu, H., Lawn, B. R. and Hsu, S. M., Hertzian contact response of tailored silicon nitride multilayers. *J. Am. Ceram. Soc.*, 1996, **79**, 1009–1014.
8. Lawn, B. R., Indentation of ceramics with spheres: a century after hertz. *J. Am. Ceram. Soc.*, 1998, **81**, 1977–1994.
9. Lee, S. K. and Lawn, B. R., Contact fatigue in silicon nitride. *J. Am. Ceram. Soc.*, 1999, **82**, 1281–1288.
10. DiGiovanni, A. A., Chan, H. M., Harmer, M. P. and Nied, H. F., Synergistic effects of porosity and glass on quasi-ductility under hertzian contact in liquid-phase-sintered alumina. *J. Am. Ceram. Soc.*, 1999, **82**, 749–752.
11. Latella, B., O'Connor, B. H., Padture, N. P. and Lawn, B. R., Hertzian contact damage in porous alumina ceramics. *J. Am. Ceram. Soc.*, 1997, **80**, 1027–1031.
12. DiGiovanni, A. A., Chan, H. M., Harmer, M. P. and Nied, H. F., Micromechanics of deformation in porous liquid-phase sintered alumina under hertzian contact. *J. Am. Ceram. Soc.*, 2001, **84**, 1844–1850.
13. Fischer-Cripps, A. C. and Lawn, B. R., Stress analysis of contact deformation in quasi-plastic ceramics. *J. Am. Ceram. Soc.*, 1996, **79**, 2609–2618.
14. Lee, S. K., Wuttiphan, S. and Lawn, B. R., Role of microstructure in Hertzian contact damage in silicon nitride: I. Mechanical characterization. *J. Am. Ceram. Soc.*, 1997, **80**, 2367–2381.
15. Gibson, L. J. and Ashby, M. F., *Cellular Solids*. Pergamon Press, Oxford, UK, 1988.